Modified Regge calculus as an explanation of dark energy

2012 Class. Quantum Grav. 29 055015

(http://iopscience.iop.org/0264-9381/29/5/055015)

IOP PUBLISHING CLASSICAL AND QUANTUM GRAVITY

Class. Quantum Grav. **29** (2012) 055015 (15pp) doi:10.1088/0264-9381/29/5/055015

Modified Regge calculus as an explanation of dark energy

W M Stuckey[1], **T J McDevitt**[2] **and M Silberstein**[3]

[1] Department of Physics, Elizabethtown College, Elizabethtown, PA 17022, USA
[2] Department of Mathematical Sciences, Elizabethtown College, Elizabethtown, PA 17022, USA
[3] Department of Philosophy, Elizabethtown College, Elizabethtown, PA 17022, USA

E-mail: stuckeym@etown.edu

Received 13 October 2011, in final form 22 January 2012
Published 17 February 2012
Online at stacks.iop.org/CQG/29/055015

Abstract

Using the Regge calculus, we construct a Regge differential equation for the time evolution of the scale factor $a(t)$ in the Einstein–de Sitter cosmology model (EdS). We propose two modifications to the Regge calculus approach: (1) we allow the graphical links on spatial hypersurfaces to be large, as in direct particle interaction when the interacting particles reside in different galaxies, and (2) we assume that luminosity distance D_L is related to graphical proper distance D_p by the equation $D_L = (1+z)\sqrt{\overrightarrow{D_p} \cdot \overrightarrow{D_p}}$, where the inner product can differ from its usual trivial form. The modified Regge calculus model (MORC), EdS and ΛCDM are compared using the data from the Union2 Compilation, i.e. distance moduli and redshifts for type Ia supernovae. We find that a best fit line through $\log\left(\frac{D_L}{\text{Gpc}}\right)$ versus $\log z$ gives a correlation of 0.9955 and a sum of squares error (SSE) of 1.95. By comparison, the best fit ΛCDM gives SSE $=$ 1.79 using $H_o = 69.2\ \text{km}\,\text{s}^{-1}\,\text{Mpc}$, $\Omega_M = 0.29$ and $\Omega_\Lambda = 0.71$. The best fit EdS gives SSE $=$ 2.68 using $H_o = 60.9\ \text{km}\,\text{s}^{-1}\,\text{Mpc}$. The best-fit MORC gives SSE $=$ 1.77 and $H_o = 73.9\ \text{km}\,\text{s}^{-1}\,\text{Mpc}$ using $R = A^{-1} = 8.38$ Gcy and $m = 1.71 \times 10^{52}$ kg, where R is the current graphical proper distance between nodes, A^{-1} is the scaling factor from our non-trivial inner product, and m is the nodal mass. Thus, the MORC improves the EdS as well as ΛCDM in accounting for distance moduli and redshifts for type Ia supernovae without having to invoke accelerated expansion, i.e. there is no dark energy and the universe is always decelerating.

PACS number: 98.80.−k

(Some figures may appear in colour only in the online journal)

1. Introduction

The problem of cosmological 'dark energy' is by now well known [1–6]. Essentially, redshifts and distance moduli for type Ia supernovae indicate that the universe is in a state of accelerated expansion when analyzed using general relativistic cosmology [7–9]. Specifically, the distance moduli increase with increasing redshift faster than predicted by general relativistic cosmology using matter alone. Until this discovery in 1998, the so-called standard model of cosmology was general relativistic cosmology with a perfect fluid stress–energy tensor and an early period of inflation. Since this leads to a decelerating expansion (except during the short, early inflationary period), something 'exotic' seemed to be required to account for the unexpectedly large distance moduli at larger redshifts, namely dark energy that causes the universe to change from deceleration to acceleration at about $z = 0.752$ [9]. The new 'standard model of cosmology', i.e. that with the most robust fit to all observational data (ΛCDM), simply adds a cosmological constant Λ to the Einstein–de Sitter cosmology model (EdS) ($\Omega_M + \Omega_\Lambda = 1$) and Λ then provides the mechanism for accelerated expansion, i.e. it provides the dark energy. The 'problem' is that our best theories of quantum physics tell us that the cosmological constant should be exactly zero [10] or something hideously large [11], and neither of these two cases holds in ΛCDM. Thus, one of the most pressing problems in cosmology today is to account for the unexpectedly large distance moduli at larger redshifts observed for type Ia supernovae [6].

The most popular attempts to explain the apparent accelerating expansion of the universe include quintessence [11–13] and inhomogeneous spacetime [1–4, 14] (there are even combinations of the two [15, 16]). Although these solutions have their critics [17], they are certainly promising approaches. Another popular attempt is the modification of general relativity (GR). These approaches, such as $f(R)$ gravity [18–23], have stimulated much debate [24–26], which is a healthy situation in science. Herein, we propose a new approach to the modification of GR via its graphical counterpart, the Regge calculus.

Specifically, we construct a Regge differential equation for the time evolution of the scale factor $a(t)$ in the EdS, and then we propose two modifications, both motivated by our work on foundational issues [27–29]. First, we allow spatial links of the Regge graph to be large (as defined below) in accord with (1) our form of direct particle interaction between sources in different galaxies and (2) the assumption that the Regge calculus is fundamental while GR is the continuous approximation thereto. Of course, direct particle interaction in its original form would require a modification to general relativistic cosmology in and of itself [30–35]. We are not concerned with saving direct particle interaction in its original form and, indeed, one need not accept our version thereof to consider the modifications of GR proposed herein, i.e. empirical motivations suffice. Second, we do not assume that luminosity distance D_L is trivially related to graphical proper distance D_p between the photon receiver and the emitter as it is in EdS, i.e. in EdS $D_L = (1 + z)d_p$ where d_p is the proper distance between the photon receiver and the emitter. There are two reasons why we do not make this assumption. First, in our view, space, time and sources are co-constructed, yet D_p is found without taking into account EM sources responsible for D_L. That is to say, in Regge EdS (as in EdS), we assume that pressureless dust dominates the stress–energy tensor and is exclusively responsible for the graphical notion of spatial distance D_p. However, even though the EM contribution to the stress–energy tensor is negligible, EM sources are being used to measure the spatial distance D_L. Second, in the continuous, GR view of photon exchange, one considers light rays (or wave fronts) in an expanding space to find $D_L = (1 + z)d_p$. In our view, there are no 'photon paths being stretched by expanding space', so we cannot simply assume $D_L = (1 + z)D_p$ as in EdS. Indeed, we find the trivial EdS relationship between luminosity distance and

proper distance holds only when D_p is small on cosmological scales. In order to generate a relationship between D_L and D_p, we turned to the self-consistency equation $KQ = J$ in our foundational approach to physics [28], where K is the differential operator, Q is the 'field'[4] and J is the source. Since we want a relationship between D_L and D_p, the 'field' of interest is a metric $h_{\alpha\beta}$ relating the graphical proper distance D_p, obtained theoretically using no EM sources, to the luminosity distance D_L, obtained observationally via EM sources. The region in question (inter-nodal region between the emitter and the receiver) has the metric $\eta_{\alpha\beta}$ given by $\mathrm{d}s^2 = -c^2\mathrm{d}t^2 + \mathrm{d}D_p^2$, so the inner product of interest can be written as $\eta_{\alpha\beta} + h_{\alpha\beta}$ where the spatial coordinate is D_p and $h_{\alpha\beta}$ is diagonal. Since each EM source proper is not 'stretched out' by the expansion of space, the spatiotemporal relationship between the emitter and the receiver is modeled per this inter-nodal region alone. Thus, unlike EdS, we have no *a priori* basis in our form of direct particle interaction to relate D_L to D_p, so we begin with the assumption $D_L = (1+z)\sqrt{\overrightarrow{D_p}\cdot\overrightarrow{D_p}} = (1+z)D_p\sqrt{1+h_{11}}$, where $\overrightarrow{D_p} = (0, D_p)$.

The specific form of $KQ = J$ that we used was borrowed from linearized gravity in the harmonic gauge, i.e. $\partial^2 h_{\alpha\beta} = -16\pi G(T_{\alpha\beta} - \frac{1}{2}\eta_{\alpha\beta}T)$. We emphasize that $h_{\alpha\beta}$ here corrects the graphical inner product $\eta_{\alpha\beta}$ in the inter-nodal region between the worldlines of the photon emitter and receiver, where $\eta_{\alpha\beta}$ is obtained via a matter-only stress–energy tensor. Since the EM sources are negligible in the matter-dominated solution, we have $\partial^2 h_{\alpha\beta} = 0$ to be solved for h_{11}. Obviously, $h_{11} = 0$ is the solution that gives the trivial relationship, but allowing h_{11} to be a function of D_p allows for the possibility that D_L and D_p are not trivially related. We have $h_{11} = AD_p + B$ where A and B are constants and, if the inner product is to reduce to $\eta_{\alpha\beta}$ for small D_p, we have $B = 0$. Presumably, A should follow from the corresponding theory of quantum gravity, so an experimental determination of its value provides a guide to quantum gravity per our view of classical gravity. As we will show, our best fit to the Union2 compilation data gives $A^{-1} = 8.38$ Gcy, so the correction to η_{11} is negligible except at cosmological distances, as expected. Essentially, we're saying the dark energy phenomenon is an indication that $A \neq 0$ so that one cannot simply assume that the distance D_L measured using EM sources corresponds trivially to the graphical proper distance D_p even though the EM sources contribute negligibly to the stress–energy tensor.

One might also ask about distance corrections per h_{00}, i.e. as regards redshift, but since redshift distances are fractions of a meter, one would not expect h_{00} to be of consequence here. Of course, there is the issue of *origin* of redshift in our approach, since typically cosmological redshift is understood to occur *between* emission and reception [36] while clearly it must occur *during* emission and reception in our view. While we do not have photons propagating through an otherwise empty space between the emitter and the receiver, we do relate the reception and emission events in null fashion through the simplices spanning the inter-nodal region between the emitter and the receiver. Using the metric in each simplex $\mathrm{d}s^2 = -c^2\mathrm{d}t^2 + \mathrm{d}D_p^2$, as above, we have $\mathrm{d}D_p = a\mathrm{d}\chi$, just as in EdS, although t is not the proper time for the nodal observers as it is in the EdS. This difference in t is accounted for in the computation of D_p where it has a small effect for the range of data in the Union2 compilation[5]. Likewise, we do not find that it leads to a significant difference in the scale factor at the time of emission a_e as a function of z for the data range in question. Not surprisingly, when we compute the redshift graphically, we find that it is equivalent to the special relativity (SR) result, i.e. $z+1 = \sqrt{\frac{(1+V_e/c)(1+V_r/c)}{(1-V_e/c)(1-V_r/c)}}$ where V_e is the velocity of the emitter at the time of emission in the (1+1)-dimensional inter-nodal

[4] The interested reader is referred to section 3 of reference [28] for an explanation of how our notion of a 'field' is consistent with our notion of direct particle interaction.

[5] There is another difference between d_p and D_p as computed using $\mathrm{d}\chi = \frac{c\mathrm{d}t}{a}$ that must be considered. This will be explained in section 2.

frame and V_r is the velocity of the receiver at the time of reception. Using this form of redshift in the EdS model and comparing the result to the use of a cosmological redshift in EdS, we find that there is no significant difference between the two results for the distance modulus μ versus redshift z well beyond the range of the Union2 compilation ($z < 2$, see figure 2). Therefore, we use the cosmological redshift $a_e = \frac{1}{1+z}$ for the computation of D_p, since the cosmological redshift is far simpler than the graphical alternative.

While these modifications are motivated by our work on foundational issues, their specific mathematical instantiations are herein aimed at explaining dark energy. Since this is our first foray into the modified Regge calculus (MORC), the specific approaches required for explaining other GR phenomena, e.g. the perihelion shift of Mercury, remain to be seen. A defense of MORC will not be undertaken here; interested readers are referred to our earlier work cited above, but a couple of comments are perhaps in order. First, the graphical lattice used herein to obtain $a(t)$ clearly violates isotropy and is not to be understood as a literal picture of the distribution of matter in the universe, e.g. galactic clusters, voids, etc. In a sense, the graphical lattice we use is no coarser an approximation than the continuum counterpart it is designed to replace, i.e. the featureless perfect fluid model of EdS where there is absolutely *no* structure. Rather, the graphical lattice simply provides a 'mean' evolution for the scale factor $a(t)$ in the equation for D_p. Second, the goal of such idealized models is to attempt to isolate 'average' geometric and/or material features of cosmology which broadly capture kinematic properties of the universe as a whole. Only when such models show some initial success are explorations into departures from their simplistic structure motivated, e.g. the inhomogeneous spacetime models cited above. Thus, the model we present herein was designed merely to test the possibility of replacing the continuous EdS cosmology with a discrete, graphical counterpart based on our form of direct particle interaction (again, for reasons unrelated to dark energy). Only upon some success of this initial test, i.e. improving the EdS fit to the type Ia supernova data, should we proceed to address the commensurate questions and implications of this approach (as outlined briefly in section 4). We believe that the results presented herein establish precisely 'some initial success' and therefore justify further exploration into this idea.

We begin in section 2 with an overview of the Regge calculus and present our temporally continuous, spatially discrete Regge EdS equation for the time evolution of the scale factor $a(t)$ and the commensurate equation for proper distance between the photon emitter and the receiver D_p in a direct inter-nodal exchange. As we will see, the spatially discrete Regge EdS equation for the time evolution of the scale factor $a(t)$ reproduces that of EdS when spatial links are small. Spatial links are 'small' when the 'Newtonian' graphical velocity v between spatially adjacent nodes on the Regge graph is small compared to c, i.e. $\left(\frac{v}{c}\right)^2 \ll 1$. In that case, the dynamics between adjacent spatial nodes is just Newtonian and the evolution of $a(t)$ in the Regge EdS is equal to that in EdS. Deviations in the evolution of $a(t)$ between the Regge EdS and MORC turn out to be small (see figure 6). Thus, the modification of Regge evolution plays a relatively minor role in the MORC fits. Rather, as we will show, the major factor in improving the EdS is $D_L = (1+z)D_p \rightarrow D_L = (1+z)\sqrt{\vec{D_p} \cdot \vec{D_p}}$. Since the Regge EdS should give the EdS when used as originally intended [37], the proposed mechanism for EM coupling in the MORC differs from that in the Regge calculus. When $v \approx 2c$, the Regge EdS encounters the 'stop point' problem [38–40], i.e. the backward time evolution of $a(t)$ halts, so $a(t)$ has a minimum and there is a maximum value of z for which one can find D_p. Of course, this is not a real problem for the Regge EdS if one is simply using it to model the EdS, since one can regularly check v in the computational algorithm and refine the size of the lattice to ensure v remains small. However, in our case, the graphical approach is fundamental, so lattice refinements are

not mere mathematical adjustments, but would constitute new 'mean' configurations of matter. Of course, such refinements are certainly required in earlier cosmological eras, but one would expect that there exists a smallest spatial scale (associated with a smallest nodal mass) so that eventually (evolving backward in time) $v \approx 2c$ could not be avoided and the minimum $a(t)$ would be reached. Thus, there are significant deviations from our use of the Regge calculus and its (originally intended) use as a graphical approximation to GR.

In section 3, we present the fits for the EdS, MORC and ΛCDM to the Union2 compilation data, i.e. distance moduli and redshifts for type Ia supernovae [41] (see figures 4 and 5). We find that the MORC improves the EdS as much as the ΛCDM in accounting for distance moduli and redshifts for type Ia supernovae even though the MORC universe contains no dark energy is therefore always decelerating. While we do not need to invoke dark energy, we do propose modifications to classical gravity. Thus, it is a matter of debate as to which approach (ΛCDM or MORC) is better.

Of course, the success of MORC in this context does not commit one to our foundational motives. In fact, one may certainly dismiss our form of direct particle interaction and simply suppose that the metric established by EM sources deviates from that of pressureless dust at cosmological distances in a graphical approach to gravity. Since motives are not germane to physics, we will not present arguments for our foundational motives here. Abandoning our motives but keeping the MORC formalism would simply result in a situation similar to that in ΛCDM where a cosmological constant is added to EdS for empirical reasons. That is, one could simply view MORC as a modification of the Regge calculus for empirical reasons without buying into our story about direct particle interaction and co-constructed space, time and sources. Motives notwithstanding, we believe our MORC formalism may provide creative new approaches to other long-standing problems, e.g. quantum gravity, unification and dark matter. We conclude in section 4 by briefly outlining future directions and challenges for this research program.

2. Overview of the Regge calculus

The Regge calculus is typically viewed as a discrete approximation to GR where the discrete counterpart to Einstein's equations is obtained from the least action principal on a 4D graph [37, 42–44]. This generates a rule for constructing a discrete approximation to the spacetime manifold of GR using small, contiguous 4D Minkowskian graphical 'tetrahedra' called 'simplices'. The smaller the legs of the simplices, the better one may approximate a differentiable manifold via a lattice spacetime (figure 1). Although the lattice geometry is typically viewed as an approximation to the continuous spacetime manifold, it could be that the discrete spacetime is fundamental while 'the usual continuum theory is very likely only an approximation' [45] and that is what we assume. Curvature in the Regge calculus is represented by 'deficit angles' (figure 1) about any plane orthogonal to a 'hinge' (triangular side of a tetrahedron, which is a side of a simplex[6]), so the curvature is said to reside on the hinges. A hinge is two dimensions less than the lattice dimension, so in 2D a hinge is a zero-dimensional point (figure 1). The Hilbert action for a vacuum lattice is $I_R = \frac{1}{8\pi}\sum_{\sigma_i \in L} \varepsilon_i A_i$ where σ_i is a triangular hinge in the lattice L, A_i is the area of σ_i and ε_i is the deficit angle associated with σ_i. The counterpart to Einstein's equations is then obtained by demanding $\frac{\delta I_R}{\delta \ell_j^2} = 0$ where ℓ_j^2 is the squared length of the jth lattice edge, i.e. the metric. To obtain equations in the presence of matter–energy, one simply adds the matter–energy action I_M to I_R and carries out the variation as before to obtain $\frac{\delta I_R}{\delta \ell_j^2} = -\frac{\delta I_M}{\delta \ell_j^2}$ [46]. The LHS becomes $\frac{\delta I_R}{\delta \ell_j^2} = \frac{1}{16\pi}\sum_{\sigma_i \in L} \varepsilon_i \cot \Theta_{ij}$ where Θ_{ij} is

[6] Our hinges are triangles, but one may use other 2D polyhedra.

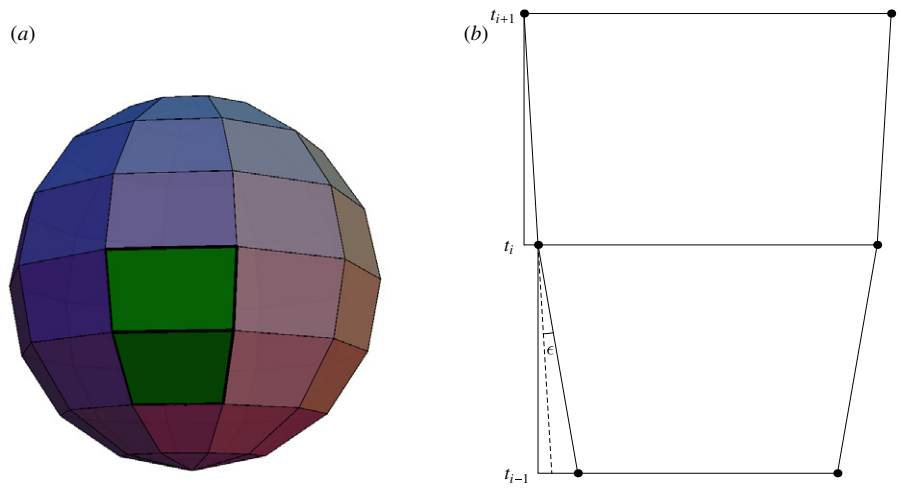

Figure 1. (*a*) Tessellated sphere and (*b*) two 'flattened' trapezoids (thick outline) from the sphere.

the angle opposite edge ℓ_j in the hinge σ_i. One finds that the stress–energy tensor is associated with lattice edges, just as the metric, and Regge's equations are to be satisfied for any particular choice of the two tensors on the lattice. The extent to which the Regge calculus reproduces GR has been studied [47–49] and general methods for obtaining Regge equations have been produced [50], but these results are of no immediate concern to us because we simply seek the Regge counterpart to a specific GR equation, i.e. a Regge differential equation for the time evolution of the scale factor $a(t)$ in EdS. Whether or not we obtain the said equation will be clear by virtue of its ability to track the analytic EdS solution in the proper regime, so we will not have to delve into issues associated with the 'accuracy' of the Regge calculus in general.

2.1. Regge EdS equation and the MORC

Following Brewin [51] and Gentle [52], we take the stress–energy associated with the worldlines of our particles to be of the form

$$\frac{12Gm}{c^2(\mathrm{i}c\Delta t)}$$

so our Regge equation is

$$\frac{12\mathrm{i}R(a_n+a_{n+1})}{c\Delta t}\frac{\left(\pi-\cos^{-1}\left(\frac{\left(\frac{R}{c}\right)^2\left(\frac{a_{n+1}-a_n}{\Delta t}\right)^2}{2\left(\left(\frac{R}{c}\right)^2\left(\frac{a_{n+1}-a_n}{\Delta t}\right)^2+2\right)}\right)-2\cos^{-1}\left(\frac{\sqrt{3\left(\frac{R}{c}\right)^2\left(\frac{a_{n+1}-a_n}{\Delta t}\right)^2+4}}{2\sqrt{\left(\frac{R}{c}\right)^2\left(\frac{a_{n+1}-a_n}{\Delta t}\right)^2+2}}\right)\right)}{\sqrt{\left(\frac{R}{c}\right)^2\left(\frac{a_{n+1}-a_n}{\Delta t}\right)^2+4}}$$

$$=\frac{12\mathrm{i}Gm}{c^3\Delta t}. \tag{1}$$

Multiplying both sides of (1) by $-\mathrm{i}c\Delta t/12$ and letting $v=R(a_{n+1}-a_n)/\Delta t$ gives

$$R(a_n+a_{n+1})\frac{\left(\pi-\cos^{-1}\left(\frac{v^2/c^2}{2(v^2/c^2+2)}\right)-2\cos^{-1}\left(\frac{\sqrt{3v^2/c^2+4}}{2\sqrt{v^2/c^2+2}}\right)\right)}{\sqrt{v^2/c^2+4}}=\frac{Gm}{c^2}. \tag{2}$$

If $\Delta t \to 0$, then v can be regarded as a 'Newtonian' velocity and $R(a_n + a_{n+1})$ can be replaced by $2r$, where r is the graphical proper distance between two adjacent vertices on the lattice. Equation (2) then becomes

$$\frac{\pi - \cos^{-1}\left(\frac{v^2/c^2}{2(v^2/c^2+2)}\right) - 2\cos^{-1}\left(\frac{\sqrt{3v^2/c^2+4}}{2\sqrt{v^2/c^2+2}}\right)}{\sqrt{v^2/c^2+4}} = \frac{Gm}{2rc^2} \tag{3}$$

which we emphasize as the unmodified Regge calculus. If $v^2/c^2 \ll 1$, then a power series expansion of the LHS of equation (3) gives

$$\frac{v^2}{4c^2} + \mathcal{O}\left(\frac{v}{c}\right)^4 = \frac{Gm}{2rc^2}. \tag{4}$$

Thus, to leading order, our Regge EdS is EdS, i.e. $\frac{v^2}{2} = \frac{Gm}{r}$, which is just a Newtonian conservation of the energy expression for a unit mass moving at escape velocity v at distance r from mass m. To better understand the relationship between the Regge EdS and EdS, we note that in EdS any comoving observer A can ask, 'What is the proper time rate of change of proper distance for the comoving observer B at a proper distance r away from me today?' The answer is precisely v given by the EdS equation $\frac{v^2}{2} = \frac{Gm}{r}$, where m is the mass contained inside the sphere of radius r centered on observer A. In EdS the matter is distributed uniformly throughout space so the mass m inside a sphere of radius r goes as r^3; thus, $v \propto r$ on spatial hypersurfaces in the EdS equation, so there is no limit to how large v is in this expression, its Newtonian. In the Regge EdS, v is the relative 'Newtonian' velocity of spatially adjacent nodes of mass m. In our view, photon exchanges occur in direct node-to-node fashion, but solving for a Regge graph between all galaxies in the universe is of course unreasonable. Instead, we use equation (3) to provide a 'mean' $a(t)$ for the computation of graphical proper distance D_p between any two photon exchangers, as in EdS, i.e.

$$\text{proper distance} = \chi_e = c\int_{t_e}^{t_o} \frac{\mathrm{d}t}{a} = c\int_{a_e}^{1} \frac{\mathrm{d}a}{a\dot{a}}. \tag{5}$$

We then compute D_p as a function of z by using equation (3) obtained from the 'mean' graph. However, before we continue there are two issues that we need to address regarding equation (5).

First, while it is true that $c\mathrm{d}t = a\mathrm{d}\chi$ for a null path in a simplex and the null path will cross all values of χ between the emitter and the receiver, the sum of $\mathrm{d}\chi = \frac{c\mathrm{d}t}{a}$ will not equal χ_e, i.e. the radial coordinate of the emitter. That is because the lines of constant χ are tilted in the simplices (figure 3), so there is a fraction of $\mathrm{d}\chi$ (given by Δ in figure 3) that is not accounted for by $\frac{c\mathrm{d}t}{a}$. This Δ is positive on the emitter's side of the simplex and negative on the receiver's side, but the Δ sum on the two sides won't cancel out exactly, since the extent of constant-χ tilt is reduced during the expansion. The correct equation for the graph is

$$\chi_e = c\int_{t_e}^{t_o} \left(1 + \frac{2V}{c}\left(\frac{\chi(t)}{\chi_e} - \frac{1}{2}\right)\right)\frac{\mathrm{d}t}{a}, \tag{6}$$

where V is the SR velocity of the emitter or receiver as a function of time and relates to our 'Newtonian' v per

$$\frac{V}{c} = \frac{v/2c}{\sqrt{1 + v^2/4c^2}}. \tag{7}$$

To simplify the analysis and obtain an estimate of how much Δ contributes, we use EdS with $z = 2$ and $H_o = 70\ \mathrm{km\,s^{-1}}$ Mpc. From EdS, we have $a(t) = \left(\frac{t}{t_o}\right)^{2/3}$, $\frac{\chi}{\chi_e} = 1 - \frac{3ct_o^{2/3}}{\chi_e}\left(t^{1/3} - t_e^{1/3}\right)$ and $\frac{v}{2c} = \frac{\chi_e}{3ct_o^{2/3}t^{1/3}}$. For $z = 2$ and $H_o = 70\ \mathrm{km\,s^{-1}}$ Mpc, we have $t_o = 9.31$ Gy, $t_e = 1.79$ Gy and

$\chi_e = 11.81$ Gcy. Using these values in equation (6), we find (iteratively) $\chi_e = 12.189$ Gcy. This increases μ (equation (13)) by 0.069 at $z = 2$ where μ is slightly greater than 44 (figure 5). This increase adds 0.0137 to $\log\left(\frac{D_L}{\text{Gpc}}\right)$ in our curve fitting, which amounts to a 1.3% increase at $z = 2$. This change is only 0.75% at $z = 0.5$ and 0.004% at $z = 0.1$. Thus, given the scatter in the data, we will ignore this correction.

Second, in the EdS, the scaling factor at emission is related to the redshift by $a_e = \frac{1}{1+z}$. In the EdS, this redshift is understood to occur while the radiation is in transit between the emitter and receiver [36]. This 'cosmological' redshift can be understood in the graphical picture to result from the fact that dt in the EdS runs along lines of constant χ and these lines are tilted away from the center of the simplex toward its nodal worldlines as discussed above (figure 3). That is, $\Delta = 0$ in the EdS so $\chi_e = \int_{t_e}^{t_o} \frac{c\,\mathrm{d}t}{a}$ holds exactly. Thus, two EdS null paths emanating from different points on a spatial link have their proper distance of separation increase from simplex to simplex. However, as explained above, our dt is perpendicular to the spatial links so the null paths of successive emissions do not increase proper distance separation when traced through the simplices, i.e. redshift occurs entirely at emission and reception. Thus, relating successive events along the emitter's worldline in a null fashion to events on the receiver's worldline, it is not surprising that we find that the time delay between successive reception events as related to the temporal spacing of the emission events is that given by SR, i.e.

$$z + 1 = \sqrt{\frac{(1 + V_e/c)(1 + V_r/c)}{(1 - V_e/c)(1 - V_r/c)}}, \tag{8}$$

where V_e is the SR velocity of the emitter at the time of emission in the (1+1)-dimensional inter-nodal frame and V_r is the SR velocity of the receiver at the time of reception. Again, these SR velocities relate to our graphical 'Newtonian' v per equation (7). As above, we simplify the analysis using the EdS equation for $a(t)$ and find $v_r = \chi_e H_o$ and $v_e = \frac{\chi_e H_o}{\sqrt{a_e}}$ where, again, χ_e is the comoving coordinate of the emitter with the receiver at the origin. We need to find $\sqrt{a_e}$ as a function of z, and then substitute into the equation for proper distance between photon exchangers in the EdS

$$d_p = \frac{2c}{H_o}(1 - \sqrt{a_e}). \tag{9}$$

Even with the simplifications, the process gets messy and ultimately was solved numerically. Since $a_o = 1$, we have $d_p = \chi_e$ (as assumed in equation (5)). Let $x = \frac{\chi_e H_o}{2c}$ and we find

$$\sqrt{a_e} = x\sqrt{\frac{(A+1)^2}{(A-1)^2} - 1}, \tag{10}$$

where

$$A = \frac{(z+1)^2(\sqrt{1+x^2} - x)}{\sqrt{1+x^2} + x}. \tag{11}$$

Thus, equation (9) is $x = 1 - x\sqrt{\frac{(A+1)^2}{(A-1)^2} - 1}$ and gives

$$A^2 - 2A + 1 - 2xA^2 + 4Ax - 2x + A^2x^2 + x^2 - 6Ax^2 = 0. \tag{12}$$

We then solve equation (12) numerically for x as a function of z and compare with the EdS version, i.e. $x = 1 - \frac{1}{\sqrt{1+z}}$ to obtain figure 2 where we see that there is no significant difference between the two results well beyond the range of the Union2 compilation ($z < 2$).

Since these two differences between the MORC and the EdS do not result in any significant difference in our fit to the data of interest, we simply use equation (5) with $a_e = \frac{1}{1+z}$ to compute D_p. However, there is one additional difference between d_p and D_p when using equation (5) that we will not ignore. We will address this additional (simple) correction in the following section where we fit the EdS, MORC and ΛCDM to the Union2 compilation.

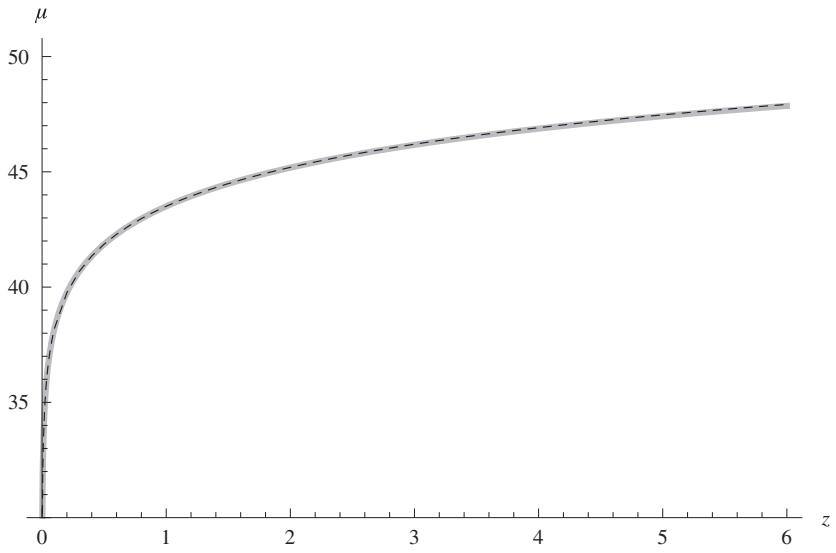

Figure 2. Comparison of the cosmological redshift (gray) and graphical special relativistic redshift (dotted) using the EdS. The two curves begin to be resolved at $z = 6$.

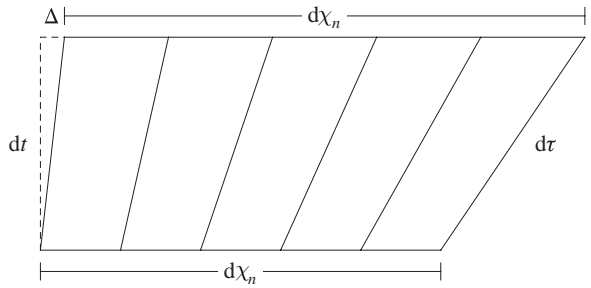

Figure 3. Lines of constant χ are tilted away from midpoint of simplex toward emitter and receiver.

3. Data analysis

The Union2 compilation provides distance modulus μ and redshift z for each supernova. In order to find μ versus z for each model, we first find the proper distance as a function of z, then compute the luminosity distance D_L, and finally

$$\mu = 5 \log \left(\frac{D_L}{10\text{pc}} \right). \tag{13}$$

For the EdS, we have equation (9) for d_p, so the only parameter in fitting the EdS is H_o. For the ΛCDM, we have $\dot{a} = H_o \sqrt{\frac{\Omega_M}{a} + \Omega_\Lambda a^2}$ where $\Omega_M + \Omega_\Lambda = 1$. Plugging this into

equation (5) we obtain

$$d_p = \frac{c}{H_o \sqrt[4]{3}\sqrt[3]{\Omega_m}\sqrt[6]{\Omega_\Lambda}}\left[F\left(\cos^{-1}\left(\frac{\sqrt[3]{\Omega_m}-\left(\sqrt{3}-1\right)\sqrt[3]{\Omega_\Lambda}}{\sqrt[3]{\Omega_m}+(\sqrt{3}+1)\sqrt[3]{\Omega_\Lambda}}\right)\middle|\frac{2+\sqrt{3}}{4}\right)\right.$$

$$\left.-F\left(\cos^{-1}\left(\frac{(z+1)\sqrt[3]{\Omega_m}-\left(\sqrt{3}-1\right)\sqrt[3]{\Omega_\Lambda}}{(z+1)\sqrt[3]{\Omega_m}+(\sqrt{3}+1)\sqrt[3]{\Omega_\Lambda}}\right)\middle|\frac{2+\sqrt{3}}{4}\right)\right], \tag{14}$$

where $F(\phi|m) = \int_0^\phi \left(1 - m\sin^2\theta\right)^{-1/2} \mathrm{d}\theta$ is the elliptic integral of the first kind. Thus, there are two fitting parameters for ΛCDM, H_o and either Ω_M or Ω_Λ. For the MORC, equation (3) gives us $a(\dot{a})$ rather than $\dot{a}(a)$, so we modify equation (5) to read

$$D_p = R\int_{b_e}^{b_1} \frac{f'(b)}{bf(b)}\sqrt{1+\frac{b^2}{4}}\mathrm{d}b, \tag{15}$$

where $b = R\dot{a}/c$,

$$f(b) = \frac{\sqrt{b^2+4}}{2\left[\pi - \cos^{-1}\left(\frac{b^2}{2b^2+4}\right) - 2\cos^{-1}\left(\frac{\sqrt{3b^2+4}}{2\sqrt{b^2+2}}\right)\right]} \tag{16}$$

and b_1 and b_e respectively solve

$$1 = \frac{Gm}{c^2R}f(b_1) \qquad \text{and} \qquad a_e = \frac{Gm}{c^2R}f(b_e).$$

The factor $\sqrt{1+\frac{b^2}{4}}$ is the correction needed to adjust the time $\mathrm{d}t$ in equation (5) to proper time $\mathrm{d}\tau$ of the nodal worldlines. (This is the 'one additional difference between d_p and D_p when using equation (5)' alluded to at the end of section 2.) Equation (5) is then solved numerically for D_p and $D_L = (1+z)D_p\sqrt{1+AD_p}$ as explained in section 1. There are three fitting parameters for the MORC, the inter-nodal coordinate R on the 'mean' graph, the nodal mass m on the 'mean' graph and A^{-1} from h_{11}. Specifying m and R is equivalent to specifying H_o in the EdS, i.e. $H_o = \sqrt{\frac{8\pi G\rho}{3}}$ in the EdS with ρ given by the graphical values of R and m per $\frac{4}{3}\pi R^3\rho = m$. Thus, compared to the EdS, the MORC (as with ΛCDM) has one additional fitting parameter A^{-1}, which presumably will be accounted for ultimately by the corresponding theory of quantum gravity.

As mentioned above, we fit these three models to the Union2 compilation data (see figures 4 and 5). In order to establish a statistical reference, we first found that a best-fit line through $\log\left(\frac{D_L}{\mathrm{Gpc}}\right)$ versus $\log z$ gives a correlation of 0.9955 and a sum of squares error (SSE) of 1.95. The EdS cannot produce a better fit than this best-fit line. The best-fit EdS gives SSE = 2.68 using $H_o = 60.9$ km s^{-1} Mpc. A current (2011) 'best estimate' for the Hubble constant is $H_o = (73.8 \pm 2.4)$ km s^{-1} Mpc [53]. Both MORC and ΛCDM produce better fits than the best-fit line with better values for the Hubble constant than the EdS. The best-fit ΛCDM gives SSE = 1.79 using $H_o = 69.2$ km s^{-1} Mpc, $\Omega_M = 0.29$ and $\Omega_\Lambda = 0.71$. This best-fit ΛCDM is consistent with its fit to the WMAP data using the latest distance measurements from BAO and a recent value of the Hubble constant [54]. The best-fit MORC (case 1, table 1) gives SSE = 1.77 and $H_o = 73.9$ km s^{-1} Mpc using $R = A^{-1} = 8.38$ Gcy and $m = 1.71 \times 10^{52}$ kg. Given the scatter in the data, the MORC and ΛCDM produce essentially equivalent fits, clearly superior to the EdS.

The 'stop point' value of z in the MORC best fit is only 2.05, so we expect the Regge evolution deviates discernibly from the EdS evolution in this trial. To check this, we compared

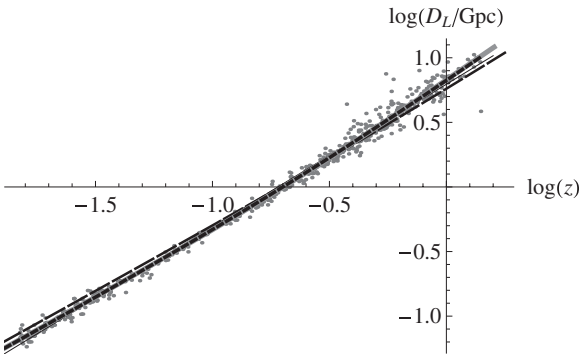

Figure 4. Plot of transformed Union2 data along with the best fits for linear regression (black), EdS (dashed), ΛCDM (gray) and MORC (dotted).

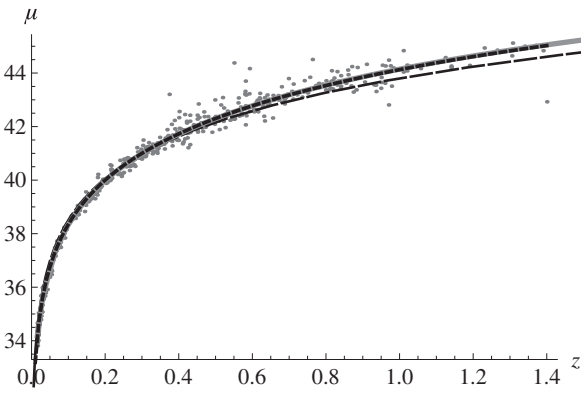

Figure 5. Plot of Union2 data along with the best fits for EdS (dashed), ΛCDM (gray) and MORC (dotted). The MORC curve is terminated at $z = 1.4$ in this figure so that the ΛCDM curve is visible.

the Regge model using the best-fit parameters and $h_{11} = 0$ with its EdS counterpart. As explained above, the EdS counterpart to a Regge graphical result is obtained by using $H_o = \sqrt{\frac{8\pi G\rho}{3}}$ in the EdS with ρ given by the graphical values of R and m per $\frac{4}{3}\pi R^3\rho = m$. The top graph in figure 6 shows that there is in fact a discernible difference between the Regge and EdS evolutions, and the EdS value of H_o obtained per R and m in this trial is 68.5 km s^{-1} Mpc, which is significantly lower than $H_o = 73.9$ km s^{-1} Mpc found in the MORC. In fact, the 20 trials with the lowest SSE values (cases 1–20, table 1) have 'stop point' z less than 10, so the Regge evolution, as distinct from the EdS evolution, does come into play. However, the Regge evolution tracks the EdS evolution when 'stop point' z is as small as 9.98 (see the bottom graph in figure 6) as is true in case 21 of table 1. And SSE = 1.78 for case 21 is still comparable to SSE = 1.79 of the best-fit ΛCDM. The only casuality in the higher 'stop point' z trials is H_o, which is lowered when Regge evolution tracks EdS evolution. However, the $H_o = 71.2$ km s^{-1} Mpc in case 21 is still comparable to $H_o = 69.2$ km s^{-1} Mpc for the best-fit ΛCDM. Thus, the Regge evolution plays a relatively minor role in the MORC fits. Since we used the cosmological redshift, $\chi_e = \int_{t_e}^{t_o} \frac{c\mathrm{d}t}{a}$, and the Regge evolution played a minor role in the MORC fits, we conclude that the major factor in improving

Table 1. Table of 35 trials that produced the best fits for the MORC. Column R is X in $R = 10^X$ m. Column ρ is X in $\rho = X \times 10^{-27}$ kg m^{-3}. Column A^{-1} is X in $A^{-1} = 10^X$ m. The other columns are self-explanatory.

	R	ρ	A^{-1}	SSE	H_o	EdS H_o	Stop point z
1	25.9	8.15	25.90	1.770 06	73.9081	65.8705	2.046 30
2	25.9	8.20	25.90	1.770 92	74.1955	66.0722	2.027 72
3	25.9	8.10	25.90	1.772 78	73.6205	65.6681	2.065 10
4	25.9	8.00	25.95	1.774 53	73.0450	65.2615	2.103 41
5	25.9	7.95	25.95	1.775 11	72.7569	65.0572	2.122 93
6	25.9	8.25	25.90	1.775 32	74.4828	66.2734	2.009 37
7	25.8	8.45	25.95	1.775 47	72.0349	67.0719	3.656 64
8	25.8	8.50	25.95	1.776 38	72.2812	67.2700	3.629 25
9	25.9	8.35	25.85	1.777 30	75.0570	66.6738	1.973 33
10	25.8	8.40	25.95	1.777 42	71.7882	66.8731	3.684 36
11	25.9	8.05	25.95	1.777 57	73.3328	65.4651	2.084 14
12	25.7	8.80	25.95	1.778 21	71.6287	68.4468	6.086 75
13	25.7	8.75	25.95	1.778 24	71.4054	68.2521	6.127 24
14	25.9	8.40	25.85	1.778 52	75.3439	66.8731	1.955 63
15	25.8	8.65	25.90	1.778 58	73.0178	67.8610	3.548 98
16	25.9	8.05	25.90	1.779 14	73.3328	65.4651	2.084 14
17	25.8	8.70	25.90	1.779 29	73.2626	68.0568	3.522 83
18	25.9	7.90	25.95	1.779 38	72.4687	64.8523	2.142 70
19	25.9	8.30	25.85	1.779 58	74.7700	66.4739	1.991 24
20	25.8	8.55	25.95	1.780 09	72.5271	67.4676	3.602 18
21	25.6	9.00	25.95	1.780 19	71.2375	69.2203	9.98215
22	25.6	8.95	25.95	1.780 53	71.0276	69.0277	10.0435
23	25.7	8.85	25.95	1.780 61	71.8515	68.6410	6.046 71
24	25.8	8.60	25.90	1.780 65	72.7726	67.6646	3.575 42
25	25.7	8.70	25.95	1.780 73	71.1816	68.0568	6.168 21
26	25.5	9.10	25.95	1.781 71	70.8743	69.6038	16.2143
27	25.5	8.90	26.00	1.781 97	70.0626	68.8347	16.6011
28	25.6	9.05	25.95	1.782 06	71.4470	69.4123	9.921 47
29	25.5	9.15	25.95	1.782 08	71.0759	69.7947	16.1202
30	25.6	8.75	26.00	1.782 09	70.1832	68.2521	10.2959
31	25.6	8.80	26.00	1.782 22	70.3950	68.4468	10.2317
32	25.4	9.00	26.00	1.782 26	69.9994	69.2203	26.5859
33	25.8	8.35	25.95	1.782 26	71.5412	66.6738	3.712 41
34	25.3	9.05	26.00	1.782 36	69.9045	69.4123	42.4792
35	25.7	8.55	26.00	1.782 37	70.5076	67.4676	6.293 96

the EdS is $D_L = (1+z)D_p \rightarrow D_L = (1+z)\sqrt{\overrightarrow{D_p} \cdot \overrightarrow{D_p}}$. Again, given the scatter of the Union2 compilation data, we consider any of the 35 MORC results in table 1, where SSE $\leqslant 1.78$ and H_o ranges (69.9 $\rightarrow$ 75.3) km s^{-1} Mpc, equivalent to the best-fit ΛCDM.

4. Discussion

We have explored a MORC approach to the EdS, comparing the result with ΛCDM using the Union2 compilation of type Ia supernova data. Our motivation for MORC comes from our approach to foundational physics that involves a form of direct particle interaction whereby sources, space and time are co-constructed per a self-consistency equation. Accordingly, since EM sources are used to measure luminosity distance D_L but are not used to compute graphical proper distance D_p, we did not expect D_p to correspond trivially to the luminosity distance D_L, i.e. we did not assume $D_L = (1+z)D_p$. Rather, we assumed a more general relationship

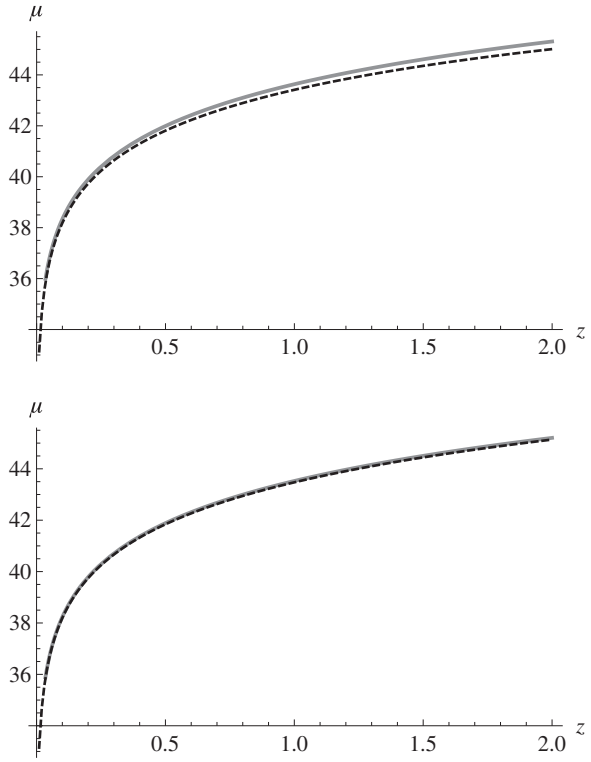

Figure 6. Top graph shows Regge evolution (dotted) without h_{11} correction and EdS evolution (gray) for case 1 in table 1 where the 'stop point' z is 2.05. The bottom graph makes the same comparison for case 21 in table 1 where the 'stop point' z is 9.98.

$D_L = (1+z)\sqrt{\overrightarrow{D_p}\cdot\overrightarrow{D_p}}$ where the inner product employed a correction to the inter-nodal graphical metric, $\eta_{\alpha\beta} \to \eta_{\alpha\beta} + h_{\alpha\beta}$ with the spatial coordinate D_p and $h_{\alpha\beta}$ diagonal, so that $D_L = (1+z)D_p\sqrt{1+h_{11}}$. The method used to find h_{11} was a form of our self-consistency equation $KQ = J$ borrowed from the homogeneous linearized gravity equation in the harmonic gauge, i.e. $\partial^2 h_{\alpha\beta} = 0$. While $h_{11} = 0$ is the solution typically used, we allowed h_{11} to be a function of D_p which gave $h_{11} = AD_p + B$ where A and B are constants. Since we wanted the inner product to reduce to $\eta_{\alpha\beta}$ for small D_p, we set $B = 0$. Our best-fit MORC (case 1, table 1) gave $A^{-1} = 8.38$ Gcy, so the correction to η_{11} is negligible except at cosmological distances, as expected.

We found that in the context of the Union2 compilation data MORC improved EdS as well as ΛCDM without having to employ dark energy. That is, the MORC universe evolves per pressureless dust and is always decelerating yet it accounts for distance moduli versus redshifts for type Ia supernovae as well as ΛCDM. Of course, this does not commit one to our foundational motives. In fact, one may certainly dismiss our form of direct particle interaction and simply suppose that the metric established by EM sources deviates from that of pressureless dust at cosmological distances; we did not present arguments for our foundational motives here. Abandoning our motives while keeping the MORC formalism would simply result in a situation similar to that in ΛCDM where a cosmological constant is added to EdS for empirical reasons, i.e. the Regge calculus was modified to account for distance moduli versus redshifts in type Ia supernovae. Motives notwithstanding, MORC's empirical success

in dealing with dark energy gives us reason to believe that this formal approach to classical gravity may provide creative new techniques for solving other long-standing problems, e.g. quantum gravity, unification and dark matter.

In order to explore this possibility, we need to check MORC against the Schwarzschild solution, where experimental data are well established and GR is well supported. While tests of the Schwarzschild solution have been conducted on spatial scales much smaller than the cosmological scales where we found a correction to EdS, it has been shown that the simplices must be small in order to reproduce the GR redshift and the perihelion precession of Mercury in the Schwarzschild solution [55, 56]. Thus, we need to verify that the MORC is consistent with the Schwarzschild solution per observational data. We might refine our study of MORC cosmology, but we feel that the easiest way to test the MORC is via the Schwarzschild solution where perhaps the issue of dark matter can be addressed in a fashion similar to dark energy in the EdS. If by chance we are able to construct a MORC for the Schwarzschild solution that passes empirical muster, we would then consider the more general issue of an action for the MORC in order to consider new approaches to quantum gravity and unification. Given the level of uncertainty involved in the next step alone, we won't speculate further.

References

[1] Garfinkle D 2006 Inhomogeneous spacetimes as a dark energy model *Class. Quantum Grav.* **23** 4811–8 (arXiv:gr-qc/0605088v2)

[2] Paranjape A and Singh T P 2006 The possibility of cosmic acceleration via spatial averaging in Lemaître–Tolman–Bondi models *Class. Quantum Grav.* **23** 6955–69 (arXiv:astro-ph/0605195v3)

[3] Tanimoto M and Nambu Y 2007 Luminosity distance-redshift relation for the LTB solution near the center *Class. Quantum Grav.* **24** 3843–57 (arXiv:gr-qc/0703012)

[4] Clarkson C and Maartens R 2010 Inhomogeneity and the foundations of concordance cosmology *Class. Quantum Grav.* **27** 124008 (arXiv:1005.2165v2)

[5] Perlmutter S 2003 Supernovae, dark energy, and the accelerating universe *Phys. Today* April 2003 53–60

[6] Bianchi E, Rovelli C and Kolb R 2010 Is dark energy really a mystery? *Nature* **466** 321–2

[7] Riess A G *et al* 1998 Observational evidence from supernovae for an accelerating universe and a cosmological constant *Astron. J.* **116** 1009–38 (arXiv:astro-ph/9805201)

[8] Perlmutter S *et al* 1999 Measurements of Ω and Λ from 42 high-redshift supernovae *Astrophys. J.* **517** 565–86

[9] Suzuki N *et al* 2011 The Hubble Space Telescope Cluster Supernova Survey: V. Improving the dark energy constraints above $z > 1$ and building an early-type-hosted supernova sample arXiv:1105.3470

[10] Carroll S 2000 The cosmological constant arXiv:astro-ph/0004075v2 (section 4)

[11] Weinberg S 2000 The cosmological constant problems arXiv:astro-ph/0005265

[12] Zlatev I, Wang L-M and Steinhardt P J 1999 Quintessence, cosmic coincidence, and the cosmological constant *Phys. Rev. Lett.* **82** 896–9

[13] Wang L M, Caldwell R R, Ostriker J P and Steinhardt P J 2000 Cosmic concordance and quintessence *Astrophys. J.* **530** 17–35

[14] Marra V and Notari A 2011 Observational constraints on inhomogeneous cosmological models without dark energy arXiv:1102.1015v2

[15] Roos M 2011 Quintessence-like dark energy in a Lemaître–Tolman–Bondi metric arXiv:1107.3028v2

[16] Buchert T, Larena J and Alimi J 2006 Correspondence between kinematical backreaction and scalar field cosmologies the 'morphon field' arXiv:gr-qc/0606020v2

[17] Zibin J P, Moss A and Scott D 2008 Can we avoid dark energy? *Phys. Rev. Lett.* **101** 251303

[18] Bernal T, Capozziello S, Hidalgo J C and Mendoza S 2011 Recovering MOND from extended metric theories of gravity arXiv:1108.5588v2 [astro-ph]

[19] Nojiri S and Odintsov S D 2010 Unified cosmic history in modified gravity: from $F(R)$ theory to Lorentz non-invariant models arXiv:1011.0544v4 [gr-qc]

[20] Kleinert H and Schmidt H J 2002 Cosmology with curvature-saturated gravitational lagrangian $r/\sqrt{1 + l^4R^2}$ *Gen. Rel. Grav.* **34** 1295–318

[21] Capozziello S 2002 Curvature quintessence *Int. J. Mod. Phys.* D **11** 483 (arXiv:gr-qc/0201033v1)

[22] Capozziello S and Francaviglia M 2008 Extended theories of gravity and their cosmological and astrophysical applications *Gen. Rel. Grav.* **40** 357–420 (arXiv:0706.1146v2)

[23] Olmo G 2011 Palatini approach to modified gravity: $f(R)$ theories and beyond *Int. J. Mod. Phys.* D **20** 413–62 (arXiv:1101.3864v1)

[24] Flanagan E E 2004 The conformal frame freedom in theories of gravitation *Class. Quantum Grav.* **21** 3817

[25] Barausse E, Sotiriou T P and Miller J C 2008 A no-go theorem for polytropic spheres in Palatini $f(R)$ gravity *Class. Quantum Grav.* **25** 062001

[26] Vollick D 2004 On the viability of the Palatini form of $1/R$ gravity *Class. Quantum Grav.* **21** 3813

[27] Stuckey W M, Silberstein M and Cifone M 2008 Reconciling spacetime and the quantum: relational blockworld and the quantum liar paradox *Found. Phys.* **38** 348–83 (arXiv:quant-ph/0510090)

[28] Stuckey W M, Silberstein M and McDevitt T 2009 Relational blockworld: a path integral based interpretation of quantum field theory arXiv:0908.4348 [quant-ph]

[29] Silberstein M, Stuckey W M and McDevitt T 2011 Being, becoming and the undivided universe: a dialogue between relational blockworld and the implicate order concerning the unification of relativity and quantum theory *Found. Phys.* submitted (arXiv:1108.2261 [quant-ph])

[30] Wheeler J A and Feynman R P 1949 Classical electrodynamics in terms of direct interparticle action *Rev. Mod. Phys.* **21** 425–33

[31] Hawking S W 1965 On the Hoyle–Narlikar theory of gravitation *Proc. R. Soc.* A **286** 313

[32] Davies P C W 1971 Extension of Wheeler–Feynman quantum theory to the relativistic domain: I. Scattering processes *J. Phys. A: Gen. Phys.* **4** 836–45

[33] Davies P C W 1972 Extension of Wheeler–Feynman quantum theory to the relativistic domain: II. Emission processes *J. Phys. A: Gen. Phys.* **5** 1025–36

[34] Hoyle F and Narlikar J V 1995 Cosmology and action-at-a-distance electrodynamics *Rev. Mod. Phys.* **67** 113–55

[35] Narlikar J V 2003 Action at a distance and cosmology: a historical perspective *Annu. Rev. Astron. Astrophys.* **41** 169–89

[36] Misner C W, Thorne K S and Wheeler J A 1973 *Gravitation* (San Francisco, CA: Freeman) p 772

[37] Regge T 1961 General relativity without coordinates *Nuovo Cimento* **19** 558571

[38] Khavari P and Dyer C C 2008 Aspects of causality in parallelisable implicit evolution scheme arXiv:0809.1815v2

[39] De Felice A and Fabri E 2000 The Friedmann universe of dust by Regge calculus: study of its ending point arXiv:gr-qc/0009093v1

[40] Lewis S M 1982 Two cosmological solutions of Regge calculus *Phys. Rev.* D **25** 306

[41] Amanullah R *et al* 2010 The supernova cosmology project: spectra and light curves of six type Ia supernovae at $0.511 < z < 1.12$ and the Union2 compilation *Astrophys. J.* **716** 712–38 (arXiv:1004.1711v1 [astro-ph])

[42] Misner C W, Thorne K S and Wheeler J A 1973 *Gravitation* (San Francisco, CA: Freeman) p 1166

[43] Barrett J W 1987 The geometry of classical Regge calculus *Class. Quantum Grav.* **4** 1565–76

[44] Williams R M and Tuckey P A 1992 Regge calculus: a brief review and bibliography *Class. Quantum Grav.* **9** 1409–22

[45] Feinberg G, Friedberg R, Lee T D and Ren H C 1984 Lattice gravity near the continuum limit *Nucl. Phys.* B **245** 343–68

[46] Sorkin R 1975 The electromagnetic field on a simplicial net *J. Math. Phys.* **16** 2432–40 , section II.F

[47] Brewin L 2000 Is the Regge calculus a consistent approximation to general relativity? *Gen. Rel. Grav.* **32** 897–918

[48] Miller M A 1995 Regge calculus as a fourth-order method in numerical relativity *Class. Quantum Grav.* **12** 3037–51

[49] Brewin L and Gentle A P 2001 On the convergence of Regge calculus to general relativity *Class. Quantum Grav.* **18** 517–26

[50] Brewin L 2010 Fast algorithms for computing defects and their derivatives in the Regge calculus arXiv:1011.1885v1

[51] Brewin L 1987 Friedmann cosmologies via the Regge calculus *Class. Quantum Grav.* **4** 899–928

[52] Gentle A P 2000 Regge geometrodynamics *PhD Thesis* Monash University, section 6.3

[53] Riess A G, Macri L, Casertano S, Lampeitl H, Ferguson H C, Filippenko A V, Jha S W, Li W and Chornock R 2011 A 3% solution: determination of the Hubble constant with the Hubble space telescope and wide field camera 3 *Astrophys. J.* **730** 119

[54] Komatsu E *et al* 2010 Seven-year Wilkinson microwave anisotropy probe (WMAP) observations: cosmological interpretation arXiv:1001.4538v3

[55] Williams R M and Ellis G F R 1981 Regge calculus and observations: I. Formalism and applications to radial motion and circular orbits *Gen. Rel. Grav.* **13** 361–95

[56] Brewin L 1993 Particle paths in a Schwarzschild spacetime via the Regge calculus *Class. Quantum Grav.* **10** 1803–23